

# The role of exchange for the spin-parallel structure factor of jellium

P. Ziesche

*Max-Planck-Institut für Physik komplexer Systeme*

*Nöthnitzer Str. 38, D-01187 Dresden, Germany*

F. Hummel

*Computational Materials Physics, University Wien*

*Sensengasse 8/12, A-1090 Wien, Austria*

(Dated: draft of December 3, 2024)

The random phase approximation (RPA) provides a qualitatively good approximation of electronic correlation in many systems. It has been successfully applied to the spin-unpolarized homogeneous electron gas (HEG) for decades, especially in the studies of its many properties such as correlation energy, momentum distribution and the spin resolved pair correlation function and structure factor. However, the RPA neglects important contributions to the spin-parallel structure factor originating from exchange effects. We derive an approximation for the spin-parallel structure factor including the lowest order exchange process beyond the RPA analytically by means of contour integration and evaluate it numerically by means of a Monte-Carlo integration. A generalized Hellmann-Feynman theorem with functional derivatives is used.

## I. INTRODUCTION

The homogeneous electron gas (HEG) has been extensively investigated at various levels of theory including quantum Monte-Carlo methods. It serves well the purpose of studying the quality of less computationally demanding approximations, such as the random phase approximation (RPA). Finite order many-body perturbation theory is useless for metallic systems, such as the HEG, since each order beyond the first one contains diverging diagrams. However, ring diagrams, such as that shown on the left of Fig. 1, can be summed to infinite order before summing over all momenta occurring in the diagrams. Macke [1] was the first who performed that renormalization and calculated what was later termed random

phase approximation. The  $1/q^{2n}$  divergence of a ring diagram in  $n$ -th order is the strongest divergence possible in that order, making the RPA ring diagrams the dominant contribution to the correlation energy at long distances or, equivalently, at high densities, meaning that the RPA becomes exact in the limit of infinite density.

All the characteristic quantities of the HEG, such as the correlation energy  $e_{\text{corr}}$ , depend on  $r_s$ , which is the radius of a sphere, containing on average just one electron. Particle number fluctuations beyond that follow from the pair-correlation functions (PCF)  $g_{a,p}$  as functions of  $r$  and (parametrically) of  $r_s$  for electron pairs with antiparallel (a) and parallel (p) spins [2]. The limiting case  $r_s = 0$  corresponds to the ideal Fermi gas. The above mentioned failure of many-body perturbation theory makes the function  $e_{\text{corr}}(r_s)$  singular at  $r_s = 0$  with  $r_s^2 \ln r_s$ .

Whereas the Coulomb hole  $g_a$ , with  $g_a(0) = 1 - \mathcal{O}(r_s)$ , arises only through the Coulomb repulsion, the larger Fermi hole  $g_p = \mathcal{O}(r^2)$  comes from the combined action of the Pauli principle and the Coulomb repulsion. Equivalent information is provided by the static structure factors (SFs)  $S_{a,p}(q)$ , which are obtained by a Fourier transform of  $g_{a,p}(r)$  [3]. An analysis in terms of Feynman diagrams shows, that  $S_a = S_d$ , whereas  $S_p$  splits according to  $S_p = S_p^{\text{HF}} + S_p^{\text{cum}}$  into a Hartree-Fock (HF) like part  $S_p^{\text{HF}}$  reducible to  $n(k)$  and a cumulant non-reducible remainder  $S_p^{\text{cum}}$  [3], which again splits according to  $S_p^{\text{cum}} = S_d - S_x$  into the direct part  $S_d$  and the corresponding exchange part  $S_x$ . Thus for  $S = S_a + S_p$  it is  $S = S_p^{\text{HF}} + 2S_d - S_x$ . These splittings have been derived in [4, 5] from the 2-body reduced density matrix and its linked-diagram representations. Here, the same splitting follows automatically from the linked-diagrams of  $e$  and the generalized Hellmann-Feynman theorem.

At the level of the RPA the  $e_{\text{corr}}$  of the HEG has been studied first by [1, 6] and in 2nd order of exchange [7]. It was extended to the static quantities  $n(k)$  [8, 9] and  $S(q)$  [10–13], to the dynamic quantities  $G(k, \omega)$ ,  $S(k, \omega)$ , and also to the 2-body reduced density matrix [4, 5]. However, the RPA neglects important contributions to the spin-parallel part of the structure factor stemming from exchange effects, such as that depicted on the right of Fig. 2(a). Here, we evaluate  $S_x$  beyond the RPA, extending it by all terms arising from the Feynman diagram shown on the right of Fig 2(b). Unlike in the second order screened exchange (SOSEX) approximation, introduced by Freeman [14], we impose no restriction on the time order, which includes particle/hole ladder diagrams.

### A. Remark on the notation

The momenta  $k = |\mathbf{k}|$  and  $q = |\mathbf{q}|$  are measured in  $k_F = 1/(\alpha r_s)$ , energies in  $k_F^2$ ,  $t(\mathbf{k}) = \mathbf{k}^2/2$ ,  $v(\mathbf{q}) = q_c^2/q^2$ ,  $q_c^2 = 4\alpha r_s/\pi$ ,  $\alpha = (4/9/\pi)^{1/3}$ ,  $\omega_{\text{pl}}^2 = q_c^2/3$ ,  $a = (1 - \ln 2)/\pi^2 = 0.0311$  is referred to as Macke number, and  $x = (\alpha r_s)^2 \ln r_s$ . There are several functions of  $q$ , often the argument is not given explicitly for convenience, e.g.  $S$  means  $S(q)$ , respectively  $S(q, r_s)$ . What is in [4] named  $(1/2)F(q)$ , is here and in [5] denoted by  $F(q)$ . Short hands: RPA=random phase approximation, SF=structure factor, PCF=pair correlation function, HF=Hartree-Fock, cum=cumulant, SR=sum rule, MC=Monte Carlo.

## II. THE STRUCTURE FACTORS

We split the structure factor  $S$  into a spin-parallel and a spin-antiparallel part  $S_{\text{p,a}}$  and do so analogously for the pair densities  $g_{\text{p,a}}$ . The SFs  $S_{\text{p,a}}$  are normalized as follows

$$\int_0^\infty d(q^3) S_{\text{a}}(q) = -[1 - g_{\text{a}}(0)], \quad \int_0^\infty d(q^3) [1 - S_{\text{p}}(q)] = 1, \quad (1)$$

and they contribute to the total interaction energy  $v = v_{\text{a}} + v_{\text{p}}$  with

$$v_{\text{a}} = \frac{3\omega_{\text{pl}}^2}{4} \int_0^\infty dq S_{\text{a}}(q), \quad v_{\text{p}} = -\frac{3\omega_{\text{pl}}^2}{4} \int_0^\infty dq [1 - S_{\text{p}}(q)] \quad (2)$$

as functions of  $r_s$ . The total energy  $e = t + v$  follows from the virial theorem  $r_s de/dr_s = v$  [15]. From the SFs  $S_{\text{a,p}}$  follow the PCFs

$$g_{\text{a}}(r) = 1 + \int_0^\infty d(q^3) \frac{\sin qr}{qr} S_{\text{a}}(q), \quad g_{\text{p}}(r) = 1 - \int_0^\infty d(q^3) \frac{\sin qr}{qr} [1 - S_{\text{p}}(q)] \quad (3)$$

with  $g_{\text{p}}(0) = g'_{\text{p}}(0) = 0$  for the Pauli principle and  $S_{\text{a,p}}(0) = 0$  from the perfect screening SR. Important correlation parameters are  $g_{\text{a}}(0)$  and  $g''_{\text{p}}(0)$ . The small- $q$  limit  $S(q \rightarrow 0) = q^2/(2\omega_{\text{pl}}) + \dots$  is the plasmon SR, see refs. in [16]. Using  $S_{\text{a,p}}$  of Eqs. (11) and (14) yields results for  $g_{\text{a,p}}$ , which qualitatively agree with Figs. 3 and 4 of [17].

The energy  $e$  is a sum of topologically distinct vacuum diagrams, each of them built up from the 1-body propagator  $G_0(\mathbf{k}, \omega)$ , which contains  $t(\mathbf{k}) = k^2/2$ , and from the static

(frequency independent) Coulomb repulsion  $v(\mathbf{q}) = q_c^2/q^2$ . The p-h-lines form closed loops, linked by interaction lines. Each interaction line comes from a p-h-line and runs into a p-h-line (forming thus vertices). Each closed loop appears twice according to the two spin orientations. Each vacuum diagram consists of closed loops linked by interaction lines defining thus a functional of  $t(\mathbf{k})$  and  $v(\mathbf{q})$ . Then  $S$  follows from the generalized Hellmann-Feynman theorem (its simple form was first found by Güttinger [18])

$$\frac{\delta e}{\delta v(\mathbf{q})} = \frac{1}{16\pi} [S(q) - 1]. \quad (4)$$

For such functional derivatives see App. A in [19]. In Eq. (4) the differential operator cuts out successively interaction lines according to the product rule. Eq. (4) generalizes the well-known relation  $v = r_s de/dr_s$  [15].

It is easy to show by means of Eq. (4) that the vacuum diagrams of  $e$  are transformed quite automatically to the 2-point diagrams of  $S_{d,x}$  and  $F$  as

$$S_a = S_d, \quad S_p = [1 - F] + [S_d - S_x] = S_p^{\text{HF}} + S_p^{\text{cum}}, \quad (5)$$

where the 'direct' diagrams  $S_d$  are as in Fig. 1 linking **two** closed loops. The exchange diagrams  $S_x$  are as in Fig. 2(a) or 2(b), where the cutting procedure happens only at **one** and the same closed loop. Fig. 2(b) represents Fig. 2(a) equivalently, but more symmetrically. In the term of Fig. 2(c) are such 2-point  $S_p$ -diagrams addressed, which have no links between its left and right half. Such  $S_p$ -diagrams can be summed up according to  $G_0 \rightarrow G$ , to give the HF-function  $F$  (with  $n(k) =$  correlated momentum distribution [4, 5, 8, 9, 20–23])

$$F(q) = \int \frac{d^3 k}{4\pi/3} n(k) n(|\mathbf{k} + \mathbf{q}|), \quad F(q \rightarrow \infty) \sim 1/q^8, \quad F_0(q) = \left[ 1 - \frac{3q}{4} + \frac{q^3}{16} \right] \Theta(2 - q). \quad (6)$$

Its Fourier transform follows from the 1-matrix in  $r$ -representation

$$f(r) = \int_0^\infty d(k^3) \frac{\sin kr}{kr} n(k) \Rightarrow \int_0^\infty d(q^3) \frac{\sin qr}{qr} F(q) = [f(r)]^2.$$

This shows, that  $S_p$  splits quite naturally into a reducible HF-part  $S_p^{\text{HF}} = 1 - F$  and a non-reducible cumulant remainder  $S_p^{\text{cum}} = S_d - S_x$  as in Eq. (5) in agreement with the linked-diagram theorem [24]:  $S_{d,x}$  are sums of linked diagrams, the unlinked ones are in the

HF term. The analog splitting of the PCF is  $g_p = g_p^{\text{HF}} + g_p^{\text{cum}}$  with

$$g_p^{\text{HF}}(r) = 1 - [f(r)]^2, \quad g_p^{\text{cum}}(r) = \int_0^\infty d(q^3) \frac{\sin qr}{qr} [S_d - S_x](q). \quad (7)$$

Similarly, the splitting of the interaction energy is  $v_p = v_p^{\text{HF}} + v_p^{\text{cum}}$  with

$$v_p^{\text{HF}} = -\frac{\omega_{\text{pl}}^2}{4} \int_0^\infty d(k^3) \int_0^\infty d(k'^3) \frac{n(k)n(k')}{|\mathbf{k} - \mathbf{k}'|^2}, \quad v_p^{\text{cum}} = \frac{3\omega_{\text{pl}}^2}{4} \int_0^\infty dq [S_d - S_x](q) \quad (8)$$

with  $v_p^{\text{HF}} \rightarrow v_1 = -(3\omega_{\text{pl}}/4)^2$  for  $r_s \rightarrow 0$ , being HF in lowest order. [The index "1" means  $v_1 \sim r_s$ .] This analysis of Eqs. (1)-(8) is in agreement with the access through the 2-body reduced density matrix [4, 5].

The asymptotics for  $q \rightarrow \infty$  is in first order (Kimball trick [10])

$$S_d = -\left(\frac{g_a(0)}{q^4} + \frac{g_p''(0)}{q^6} + \dots\right) \omega_{\text{pl}}^2 + \dots, \quad S_x = -\left(\frac{g_a(0)}{q^4} + \frac{4g_p''(0)}{q^6} + \dots\right) \omega_{\text{pl}}^2 + \dots. \quad (9)$$

With Eq. (5) it is  $S_a = S_d$  and  $S_p = 1 + [S_d - S_x] + \dots$  or  $S_p = 1 + (3g_p''(0)/q^6) \omega_{\text{pl}}^2 + \dots$ , see [12]. So  $S_p(q \rightarrow \infty)$  starts with a  $1/q^6$ -term, while the total SF  $S = S_a + S_p$  starts with a  $1/q^4$ -term, approaching zero from below. The quantities  $1 - g_a(0) = 0.7317 r_s + \dots$  [11] and  $2/5 - g_p''(0) = 0.2291 r_s + \dots$  [13] are correlation measures, vanishing for  $r_s \rightarrow 0$  and increasing with  $r_s$ . For  $r_s \rightarrow 0$  the correlation induced cumulant parts vanish and it remains (the uncorrelated) HF in lowest order:

$$S_p^{\text{HF}} \rightarrow S_0(q) = \left(\frac{3q}{4} - \frac{q^3}{16}\right) \Theta(2-q) + \Theta(q-2), \quad g_p^{\text{HF}} \rightarrow g_0(r) = 1 - \left(\frac{3(-r \cos r + \sin r)}{r^3}\right)^2. \quad (10)$$

The cusp singularities  $S_0(q \rightarrow 0) \sim q$  and  $\sim q^3$  make the non-oscillatory asymptotic terms of  $g_0(r \rightarrow \infty) \sim 1/r^4$  and  $\sim 1/r^6$  [25].

To gain information from the above Eqs. (1)-(10) the SFs  $F, S_{d,x}$  need to be known at least approximately. For  $S_{d,x}$  this is done within the RPA.

### A. Antiparallel-spin pairs: Coulomb hole in RPA

Fig. 1 shows the contribution to  $S_a$  in the lowest order of RPA:

$$S_{\text{ar}}(q) = -\frac{(3\omega_{\text{pl}})^2}{4\pi} 2q \int_0^\infty du \frac{R^2(q, u)}{q^2 + q_c^2 R(q, u)}, \quad S_a = S_{\text{ar}} + \dots. \quad (11)$$

Fig. 3 shows  $S_a$  as a function of  $q$  and  $r_s$ . The index r denotes the RPA and the dots mean terms beyond RPA. Asymptotic properties: It has the small- $q$  asymptotics

$$S_a(q \rightarrow 0) = -\frac{1}{2} \cdot S_0(q) + \frac{1}{2} \cdot \frac{q^2}{2 \omega_{\text{pl}}} + \left[ d_4 \left( \frac{q}{\omega_{\text{pl}}} \right)^4 + d_5 \left( \frac{q}{\omega_{\text{pl}}} \right)^5 + \dots \right] \omega_{\text{pl}} + \dots \quad (12)$$

with the  $r_s$ -independent linear-cubic or ideal-gas term  $S_0$  of Eq. (10) and with a plasmon term  $\sim q^2$  (more precisely one half of it, the other half comes from  $S_p$ ). The  $r_s$ -dependent coefficients are in agreement with the bounds estimated by Iwamoto [26]. For  $r_s \approx 5$  it is  $d_4 \approx -0.0748$  and  $d_5 \approx +0.024$ .  $S_a(0) = 0$  corresponds to the perfect screening SR.  $S_a$  of Eq. (11) has the large- $q$  asymptotics  $\sim -(1/q^4 + 0.4/q^6 + \dots)$  as  $S_x$ . But cusp and curvature theorems demand a decoration by correlation parameters according to Eq. (9).

Integral properties:  $S_a$  determines the antiparallel-spin PCF  $g_a$ , in particular the norm of  $S_a = S_d$  fixes the near-field correlation parameter  $g_a(0)$  in RPA [according to Eq. (1), respectively Eq. (3) for  $r = 0$ ].  $S_{ar}$  of Eq. (11) in the interaction energy  $v_a$  of Eq. (2) gives

$$v_{ar} = -\frac{1}{2} \cdot \frac{27 \omega_{\text{pl}}^4}{8\pi} \int_0^\infty du \int_0^\infty d(q^2) \frac{R^2(q, u)}{q^2 + q_c^2 R(q, u)}. \quad (13)$$

For  $r_s \rightarrow 0$ , this behaves as  $v_a \rightarrow a \cdot x + \dots$  [with  $a = (1 - \ln 2)/\pi^2$  and  $x = (\alpha r_s)^2 \ln r_s$ ].

## B. Parallel-spin pairs: Fermi hole beyond RPA

The exchange term  $S_x$  is part of the Fermi hole  $S_p$ , as seen from Eq. (5). The formula corresponding to Fig. 2(a) yields after a tedious derivation with contour integrations (P.Z.):

$$S_{xr}(q) = -3 \int \frac{d^3 k_1 d^3 k_2}{(4\pi)^2} \int_{-\infty}^{+\infty} \frac{k}{\pi} \frac{du}{(k^2 u^2 + \varepsilon_1^2)(k^2 u^2 + \varepsilon_2^2)} \cdot \frac{q_c^2}{k^2 + q_c^2 R(k, u)}, \quad (14)$$

with  $k_{1,2} < 1 < |\mathbf{k}_{1,2} + \mathbf{q}|$ ,  $\mathbf{k} = \mathbf{k}_1 + \mathbf{k}_2 + \mathbf{q}$ ,  $\varepsilon_1 = t(\mathbf{k}_2 + \mathbf{q}) - t(\mathbf{k}_1)$ ,  $\varepsilon_2 = t(\mathbf{k}_1 + \mathbf{q}) - t(\mathbf{k}_2)$ , and  $t(\mathbf{k}) = \mathbf{k}^2/2$ . One way to check this complicated integral is, to remove the screening term  $R(q, u)$  in the denominator. This yields the well-known energy denominator for the exchange term in lowest order,

$$S_{x1}(q) = -\frac{\omega_{\text{pl}}^2}{(4\pi/3)^2} \int \frac{d^3 k_1 d^3 k_2}{\mathbf{q} \cdot (\mathbf{k}_1 + \mathbf{k}_2 + \mathbf{q})} \frac{1}{(\mathbf{k}_1 + \mathbf{k}_2 + \mathbf{q})^2} \quad (15)$$

with  $k_{1,2} < 1 < |\mathbf{k}_{1,2} + \mathbf{q}|$ , as it should. This result strengthens the confidence in the correctness of Eq. (14). The exchange integral (15) has been calculated by Gutlé and

Cioslowski [5, 27]. From (15) follows

$$S_{x1}(q \rightarrow 0) = -\frac{3}{4\pi}(2 \ln 2 - 1) r_s q + \dots$$

With  $S_x$  also  $g_p^{\text{cum}}$  and  $v_c^{\text{cum}}$  are available, see Eqs. (7) and (8).

Unfortunately the integral (14) is not known so far as an explicit function of  $q$  and  $r_s$ . It can, however, be evaluated numerically by means of a Monte Carlo integration. We first draw uniformly distributed momenta  $\mathbf{k}_1$  and  $\mathbf{k}_2$  such that  $|\mathbf{k}_{1,2}| < 1 < |\mathbf{k}_{1,2} + \mathbf{q}|$ . Subsequently, we integrate over  $u$  for each sampled pair  $\mathbf{k}_{1,2}$  with a weighted Gauss-Kronrod rule using the term  $\varepsilon_1 \varepsilon_2 / (k^2 u^2 + \varepsilon_1^2)(k^2 u^2 + \varepsilon_2^2)$  as the weighting function since it can be integrated analytically. For each value of  $q$  we find 15 and 40000 samples sufficient for the frequency integration and momentum integration, respectively. Fig. 4 shows the exchange structure factor as a function of  $q$  for different values of  $r_s$ . The error bars give the 95% confidence interval estimated from the variance of the integrand. The statistical uncertainty of the variance is in turn estimated using the fourth central statistical moment.

The results for  $S_x$  vs.  $q$  are shown in Fig. 4. The  $S_x$  of Eq. (14) violates the large- $q$  behavior by showing 1 and 2/5 instead of the correlation parameters  $g_a(0)$  and  $g_p''(0)$ , respectively. For  $S_p$  with Eqs. (6) and (10) it holds for  $q \rightarrow \infty$

$$S_p = 1 + \left( \frac{3g_p''(0)}{q^6} + \dots \right) \omega_{\text{pl}}^2 + \dots \Rightarrow S = 1 - \left( \frac{g_a(0)}{q^4} - \frac{2g_p''(0)}{q^6} + \dots \right) \omega_{\text{pl}}^2 + \dots, \quad (16)$$

where the on-top-Fermi-hole curvature  $g_p''(0)$  comes from

$$g_p''(0) = \frac{4}{3}t - \int_0^\infty dq q^4 [S_d - S_x](q), \quad \int_0^\infty d(q^3) [S_d - S_x](q) = 0. \quad (17)$$

see Appendix A in [5].  $S_{d,x}$  approach zero asymptotically from below and they are equally normalized. The small- $q$  behavior of  $S_x$  and of  $S_p = [1 - F] + [S_d - S_x]$  are not known so far. If one considers Eq. (12) and splits  $F$  according to  $1 - F = 1 - F_0 - \Delta F = S_0 - \Delta F$  into an ideal-gas term  $F_0$  and an  $r_s$ -dependent, i.e. a correlation induced remainder  $\Delta F$ , then it seems to move with

$$S_p = S_0 + S_d - [S_x + \Delta F] = \frac{1}{2} \cdot S_0 + \frac{1}{2} \cdot \frac{q^2}{2\omega_{\text{pl}}} - [S_x + \Delta F] + \dots \quad (18)$$

in the right direction, because the total SF  $S = S_a + S_p = 0 + q^2/(2\omega_{\text{pl}}) + \dots$  seems to obey the plasmon SR (thereby cancelling the  $r_s$ -independent ideal-gas terms  $S_0$ .) How  $[S_x + \Delta F](q)$  behaves for  $q = 0$ , respectively  $q \rightarrow 0$ , remains to be studied.

According to [1, 15] the high-density limits in lowest order of RPA

$$e = t_0 + v_1 + a \cdot x + \dots \quad \text{and} \quad v = v_1 + 2a \cdot x + \dots \quad (19)$$

hold [with  $a = (1 - \ln 2)/\pi^2$  and the shorthand  $x = (\alpha r_s)^2 \ln r_s$ ]. On the other hand it is  $v = v_a + v_p$  with Eqs. (2) and (13) and  $v_a = a \cdot x + \dots$ . This lets expect  $v_p \rightarrow v_1 + a \cdot x + \dots$  for  $r_s \rightarrow 0$ . Indeed, with the above splitting  $F = F_0 + \Delta F$  and the above total-energy correlation term  $e_{\text{corr}} \rightarrow a \cdot x + \dots$  it turns out  $v_p \rightarrow v_1 + a \cdot x + \dots$  for  $r_s \rightarrow 0$ , supposed it is  $\int_0^\infty dq [S_x + \Delta F](q) = 0$ . [Again the need appears, to study the  $q$ -function  $S_x + \Delta F$ .]

### III. SUMMARY

For the pair correlation function or structure factor (SF) one has to distinguish electron pairs with antiparallel (a) and and parallel (p) spins. The spin-antiparallel SF  $S_a$  is within RPA wellknown. The spin-parallel SF  $S_p$  proves to be a sum of a reducible HF-like term  $S_p^{\text{HF}}$  and a non-reducible cumulant remainder  $S_p^{\text{cum}}$ . This  $S_p^{\text{cum}}$  contains - besides  $S_a = S_d$  an exchange term  $S_x$ , here for the first time calculated analytically (contour integrations) and numerically (Monte-Carlo method).

If  $n(k)$  is available, then  $t$  and  $S_p^{\text{HF}} = S_0 + \dots$  can be calculated with  $v_p^{\text{HF}} = v_1 + \dots$  and  $g_p^{\text{HF}} = g_0 + \dots$ . If  $S_d$  is available, then  $v_a$  and  $g_a$  in particular  $g_a(0)$  can be calculated. If  $S_x$  is available, then  $S_p^{\text{cum}} = S_d - S_x$ ,  $g_p^{\text{cum}}$ ,  $g_p = g_p^{\text{HF}} + g_p^{\text{cum}}$ , in particular  $g_p''(0)$ , and  $v_p^{\text{cum}}$ ,  $v_p = v_p^{\text{HF}} + v_p^{\text{cum}}$ ,  $v = v_a + v_p$  and  $e = t + v$  and  $e_{\text{corr}} = e - t_o - v_1$  can be calculated, hopefully obeying the Lieb-Oxford bound  $e_{\text{corr}} \geq B v_1$  with  $B = 1, \dots, 1.93$  for  $r_s = 0, \dots, \infty$  [28, 29] and refs. therein. When going through these steps, MC results [30] should be incorporated similar as in [16]. Whereas the singular behavior of  $n(k)$  for  $k \rightarrow 1^\pm$  is known (in RPA), the special behavior of  $S_{d,x}(q)$  for  $q \rightarrow 2^\pm$  [curvature jump, responsible for the  $r_s$ -dependent Friedel oscillations of  $g_{a,p}(r)$ ] is not known so far.

Quite another question is, how the analysis presented here applies to recent attempts to split the Coulomb electron-electron repulsion into a short-range and a long-range part, see [31, 32] and to use different approximations for these long- and short-range contributions to the exchange and correlation energy.

### Acknowledgment

The authors acknowledge P. Fulde and the Max Planck Institute for the Physics of Complex Systems Dresden for supporting this work and we thank the  $\Psi_{\mathbf{k}}$  community for helping to build fruitful cooperation as well as the DPG for their exciting Spring Meetings Dresden 2014 and Berlin 2015. Thanks also to J. Cioslowski, P. Gori-Giorgi, J.P. Perdew, and A. Savin for stimulating discussions.

---

- [1] W. Macke, Z. Naturforsch. A **5**, 192 (1950). Another approach with the same result is due to D. Bohm and D. Pines (1953).
- [2] P. Ziesche, J. Tao, M. Seidl, and J.P. Perdew, Int. J. Quantum Chem. **77**, 819 (2000).
- [3] For the history of the cumulant concept in Statistical Physics and Many-Body theory see e.g. P. Ziesche and refs. therein in J. Cioslowski (Ed.), Many-Electron Densities and Density Matrices, p. 34, Kluwer/Plenum, New York (2000).
- [4] P. Ziesche, Phys. Rev. A **86**, 012508 (2012); A **89**, 059902(E)(2014).
- [5] P. Ziesche and J. Cioslowski, J. Modern Phys. **5**, 725 (2014). - The paragraph with Eq. (4.11) proves to be omitted.
- [6] M. Gell-Mann and K. Brueckner, Phys. Rev. **106**, 364 (1957).
- [7] L. Onsager, L. Mittag, and M. J. Stephen, Ann. Physik (Leipzig) **18**, 71 (1966).
- [8] E. Daniel and S.H. Vosko, Phys. Rev. **120**, 2041 (1961).
- [9] I.O. Kulik, Zh. Éksp. Teor. Fiz. **40**, 1343 (1961) [Sov. Phys. JETP **13**, 946 (1961)].
- [10] J.C. Kimball, Phys. Rev. A **7**, 1648 (1973).
- [11] J.C. Kimball, Phys. Rev. B **14**, 2371 (1976).
- [12] A.K. Rajagopal, J.C. Kimball, M. Banerjee, Phys. Rev. B **18**, 2339 (1978).
- [13] V.A. Rassolow, J.A. Pople, and M.A. Ratner, Phys. Rev. B **59**, 2232 (2000).
- [14] D. Freeman, Phys. Rev. B **15**, 5512 (1977).
- [15] N.H. March, Phys. Rev. **110**, 604 (1958).
- [16] P. Gori-Giorgi, F. Sacchetti, G.B. Bachelet, Physica A **280**, 199 (2000); Phys. Rev. B **61**, 7353 (2000); Phys. Rev. B **66**, 159901(E)(2002).
- [17] P. Ziesche, Int. J. Quantum Chem. **90**, 342 (2002).

- [18] P. Güttinger, Z. Phys. **73**, 169 (1932).
- [19] P. Ziesche, Ann. Physik (Berlin) **522**, 739 (2010).
- [20] P. Gori-Giorgi and P. Ziesche, Phys. Rev. B **66**, 235116 (2002).
- [21] V. Olevano et al., Phys. Rev.B **86**, 195123 (2012).
- [22] M. Holzmann et al., Phys. Rev. Lett. **107**, 110402 (2011).
- [23] S. Huotari et al., Phys.Rev.Lett. **105**, 086403 (2010).
- [24] P. Ziesche, Commun. Math. Phys. **5**, 191 (1967).
- [25] P. Ziesche, phys. stat. sol. (b) **242**, 2051 (2005).
- [26] N. Iwamoto, Phys. Rev. A **33**, 1940 (1986), Eq. (4.2)
- [27] C. Gutlé, Comp. Phys. Commun. **174**, 836 (2006). The marked simplification for  $q \geq 2$  is due to J. Cioslowski [5].
- [28] E.H. Lieb and S. Oxford, Int. J. Quantum Chem. **19**, 427 (1981).
- [29] J.P. Perdew et al., J. Chem. Phys. **140**, 18A533 (2014).
- [30] D.M. Ceperley, Phys. Rev. B **18**, 3126 (1978); D.M. Ceperley and B.J. Alder, Phys. Rev. Lett. **45**, 566 (1980).
- [31] P. Gori-Giorgi and A. Savin, Phys. Rev. A **73**, 032506 (2006).
- [32] A. Savin, Chem. Phys. **356**, 91 (2009).

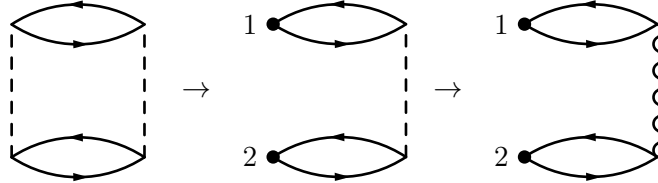


FIG. 1: Direct vacuum diagram of second order. The first step cuts out the left interaction line. The second step brings RPA screening of the right interaction line.

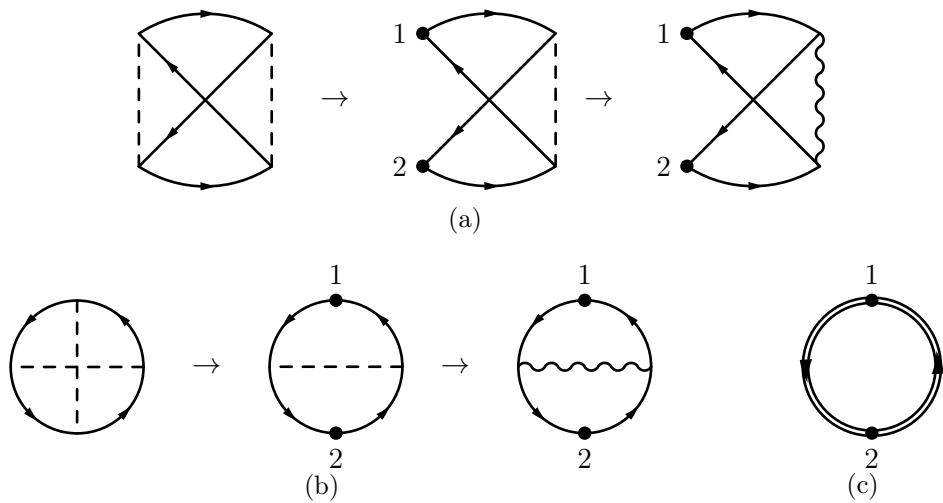


FIG. 2: (a) Exchange vacuum diagram of second order corresponding to the direct diagrams of Fig. 1. The first step cuts out the left interaction line. The second step brings RPA screening of the right interaction line. (b) The same diagrams of (a), but more symmetrically represented. (c) In this term there are no links between the left and the right half. They can be summed up to give the HF-function  $F(q)$ .

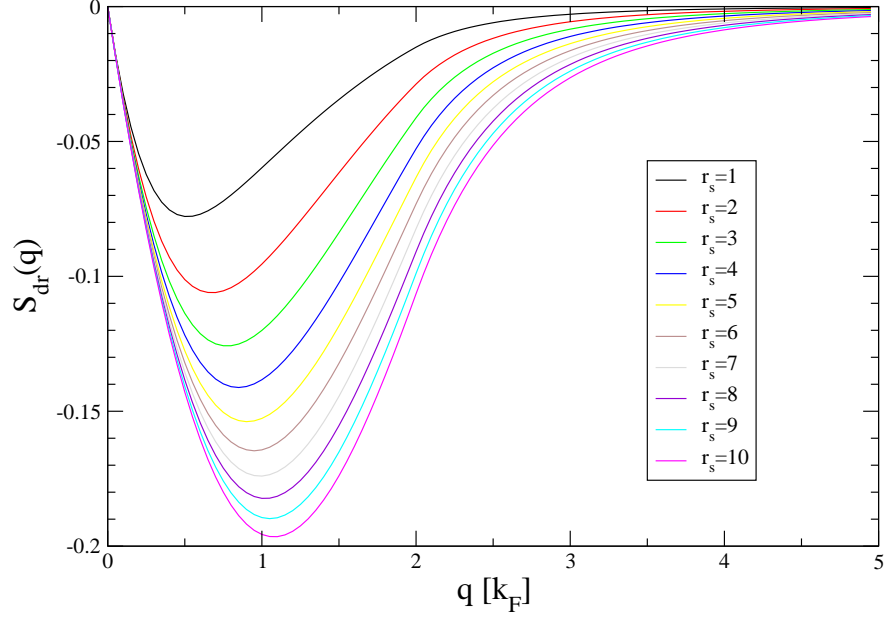


FIG. 3: Direct structure factor in RPA according to Eq. (11) from the diagrams in Fig. 1. Note  $S_a = S_d$ .

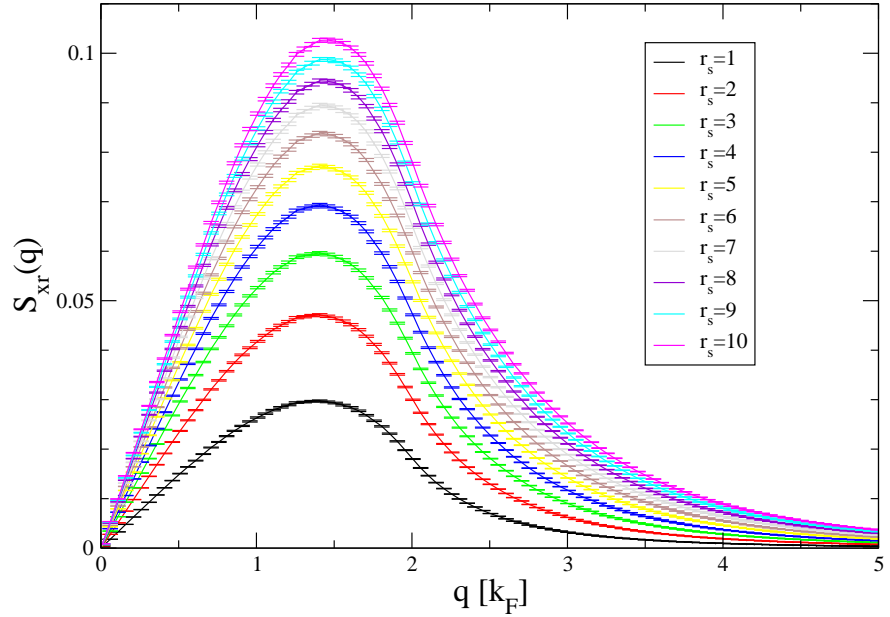


FIG. 4: Exchange structure factor in RPA  $S_x(q)$  according to Eq. (14) from the diagrams in Fig. 2(a). Note  $S_p = S_p^{\text{HF}} + S_p^{\text{cum}}$  and  $S_p^{\text{cum}} = S_d - S_x$ . The error bars show the 95% confidence interval of the MC integration.